High Reduction Efficiencies of Adsorbed NO$_x$ in Pilot-Scale Aftertreatment Using Nonthermal Plasma in Marine Diesel-Engine Exhaust Gas

Takuya Kuwahara [1,*] **, Keiichiro Yoshida** [2] **, Tomoyuki Kuroki** [3] **, Kenichi Hanamoto** [4] **, Kazutoshi Sato** [4] **and Masaaki Okubo** [3]

[1] Department of Mechanical Engineering, Nippon Institute of Technology, 4-1 Gakuendai, Miyashiro-machi, Minamisaitama, Saitama 345-8501, Japan

[2] Department of Electrical and Electronic Systems Engineering, Osaka Institute of Technology, 5-16-1 Omiya, Asahi-ku, Osaka 535-8585, Japan; keiichiro.yoshida@oit.ac.jp

[3] Department of Mechanical Engineering, Osaka Prefecture University, 1-1 Gakuen-cho, Naka-ku, Sakai 599-8531, Japan; kuroki@me.osakafu-u.ac.jp (T.K.); mokubo@me.osakafu-u.ac.jp (M.O.)

[4] Daihatsu Diesel MFG. Co., Ltd., 45 Amura-cho, Moriyama city, Shiga 524-0035, Japan; kenichi.hanamoto@dhtd.co.jp (K.H.); kazutoshi.sato@dhtd.co.jp (K.S.)

* Correspondence: takuya.k@nit.ac.jp; Tel.: +81-480-33-7719

check for
updates

Abstract: An efficient NO$_x$ reduction aftertreatment technology for a marine diesel engine that combines nonthermal plasma (NTP) and NO$_x$ adsorption/desorption is investigated. The aftertreatment technology can also treat particulate matter using a diesel particulate filter and regenerate it via NTP-induced ozone. In this study, the NO$_x$ reduction energy efficiency is investigated. The investigated marine diesel engine generates 1 MW of output power at 100% engine load. NO$_x$ reduction is performed by repeating adsorption/desorption processes with NO$_x$ adsorbents and NO$_x$ reduction using NTP. Considering practical use, experiments are performed for a larger number of cycles compared with our previous study; the amount of adsorbent used is 80 kg. The relationship between the mass of desorbed NO$_x$ and the energy efficiency of NO$_x$ reduction via NTP is established. This aftertreatment has a high reduction efficiency of 71% via NTP and a high energy efficiency of 115 g(NO$_2$)/kWh for a discharge power of 12.0 kW.

Keywords: aftertreatment; energy efficiency; marine diesel engine; nonthermal plasma; NO$_x$

1. Introduction

The advantages of diesel engines are low CO$_2$ emissions and high fuel efficiency with respect to the output power. In general, ships use diesel engines as propulsion and auxiliary engines because various types of fuels can be employed. However, their emissions contain harmful particulate matter (PM) and NO$_x$ (NO + NO$_2$). Therefore, exhaust purification requires aftertreatment technologies [1]. These technologies have been extensively studied and developed in recent years, e.g., in our previous studies [2,3].

Reduction of NO$_x$ from diesel emissions is difficult. However, emissions requirements have become increasingly stringent in recent years. The improvement of fuel injection in these engines has been investigated [4]. To reduce NO$_x$ emissions in O$_2$-rich environments, selective catalytic reduction (SCR) using urea solution or ammonia has been utilized [5–11]. Some methods combine SCR with nonthermal plasma (NTP) [12–16]. However, SCR requires a high temperature of 300 °C for catalyst activation, and there are issues regarding the production of nanoparticles, leakage of harmful ammonia, use of

harmful heavy-metal SCR catalysts, and storage of the urea solution. Additionally, NO_x reduction technologies using NTP without a catalyst have been investigated [17,18].

Marine diesel engines are the next target of regulations. Normally, NO_x concentrations in the emissions of marine diesel engines are relatively high (500–1000 ppm), and the emissions contain SO_x (typically 100 ppm) in addition to PM [2].

The regulations that govern marine diesel engines are specified by the International Maritime Organization (IMO) as explained for a rotation speed of 900 rpm in [2]. In these regulations, the emission is restricted by the mass of NO_x emitted per unit of engine output energy for a given engine rotation speed, and is divided into Tiers I, II, and III according to the enforcement period. For a marine diesel engine with a rotation speed of 900 rpm, which is the target engine type in this study, NO_x emissions should be <11.5 g/kWh for Tier I in 2000, 9.20 g/kWh for Tier II in 2011, and 2.31 g/kWh in a NO_x-regulated emission area for Tier III in 2016. Therefore, a NO_x reduction of 6.89 g/kWh is required from Tier II to the current Tier III applied in 2016. This corresponds to a 75% reduction. Given the importance of NO_x emissions, more stringent regulations may be imposed on marine diesel engines in the future, which could require a similar amount of NO_x reduction.

Considering the circumstances of marine diesel emission and the emission regulations, NO_x treatment, as well as the removal of PM, must be urgently addressed [19–22]. In 2011, the main manufacturers of marine diesel engines were able to successfully satisfy the Tier II NO_x emission standards via combustion improvements. However, to satisfy the more stringent Tier III, an effective aftertreatment technology is indispensable. Urea-SCR technology is presently the most promising approach. However, it requires the storage of large amounts of urea solution inside the vessels. NO_x reduction via wet scrubbing using a chemical solution has also been investigated [23]. However, it requires a tank of chemical solution in the ship, which has limited space.

In this study, an aftertreatment technology for NO_x reduction and PM treatment using NTP for a marine diesel engine is developed on the basis of our previous studies in a laboratory-scale experiment [24,25]. Considering practical use, experiments are performed for a larger number of cycles compared with our previous study to obtain more data. The objective is to obtain a more accurate relationship between the mass of desorbed NO_x and the mass of NO_x reduced by NTP with the data. The amount of adsorbent is 80 kg. Compared with SCR, this technology offers the advantages of eliminating the requirement of urea solution or harmful heavy-metal catalysts and operation at a temperature of <150 °C. In our previous investigation [3], PM and NO_x reductions were studied in the aftertreatment for a marine diesel engine with an output power of 610 kW. In another one of our previous studies [2], NO_x reduction with NO_x adsorbents unused in the aftertreatment was investigated for a marine diesel engine with an output power of 1071 kW. In the present study, according to the results of our previous investigations regarding NO_x reduction [2], experiments involving aftertreatment for a marine diesel engine with an output power of 1071 kW are repeated for a longer period (up to 19 cycles). In the aftertreatment, estimation of the NO_x reduction efficiency is significant for the design and operation of the system. Compared with the previous studies, considerably more data are obtained to provide a highly accurate estimation of the efficiency of NO_x reduction via NTP.

2. Operating Principle of NO_x Reduction in Aftertreatment

In the previously reported technology [2,24,25], given that NO_x cannot be efficiently and directly reduced by NTP under O_2-rich conditions, it is first adsorbed by adsorbents under O_2-rich conditions. After the adsorption, NO_x is desorbed by heating the adsorbents under O_2-lean (preferably O_2 < 2%) and fuel-rich (CO and hydrocarbon-rich) gaseous conditions. Switching the different processes is achieved by changing the exhaust path flows and by using the waste-heat recovery of the engine. The high-concentration NO_x desorbed from the adsorbents is effectively reduced to N_2 and N radicals by NTP. O_2-lean or N_2 gaseous conditions can be achieved using an O_2 penetration membrane or by controlling the engine operating mode (fuel-injection mode). The following chemical reaction for NO_x reduction is performed under O_2-lean conditions with NTP:

$$2NO_x + 2N \rightarrow 2N_2 + xO_2 \ (>\text{room temperature}). \tag{1}$$
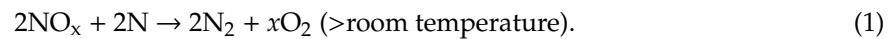
The NTP reactors should only be turned on when high concentrations of NO_x are desorbed and only during the short desorption period, reducing the required plasma energy. Laboratory-scale experiments based on this procedure in which NO_x was treated with a high energy efficiency were reported in our previous papers [26–29], and a related patent was filed [30].

Figure 1 shows process diagrams of the PM and NO_x simultaneous reduction system for a marine diesel engine. Because the objective of the present study is to investigate the NO_x reduction efficiencies in a larger number of cycles compared with our previous study [2], the experimental setup and processes are the same. The system mainly consists of the marine diesel engine, diesel particulate filters (DPFs), an adsorption chamber, and NTP reactors. PM reduction is first performed with a pair of DPFs, and the DPFs are regenerated via ozone injection. Next, NO_x reduction is achieved through two flow processes: an adsorption process followed by a desorption process combined with the NTP reaction. The sequential application of these two processes in the same adsorption chamber realizes continuous NO_x reduction. In the adsorption process, the flow rate of the exhaust gas determines the flow velocity, which is measured by pitot tubes. After the exhaust gas is cooled using a water-cooling-type cooler, it passes through the adsorption chamber, where NO_x is adsorbed by adsorbents. The NO_x concentrations are measured at the inlet and outlet of the chamber. In the desorption process, the exchanged waste heat is added to the adsorbent pellets via a heat exchanger to induce the thermal desorption of NO_x. Simultaneously, N_2 gas flows over the packed adsorbent pellets. Then, high concentrations of NO_x are desorbed from the chamber. The desorbed NO_x is reduced in the NTP reactor. Thus, the simultaneous reduction of PM and NO_x is achieved [2]. In the next section, the experimental apparatus and results are presented.
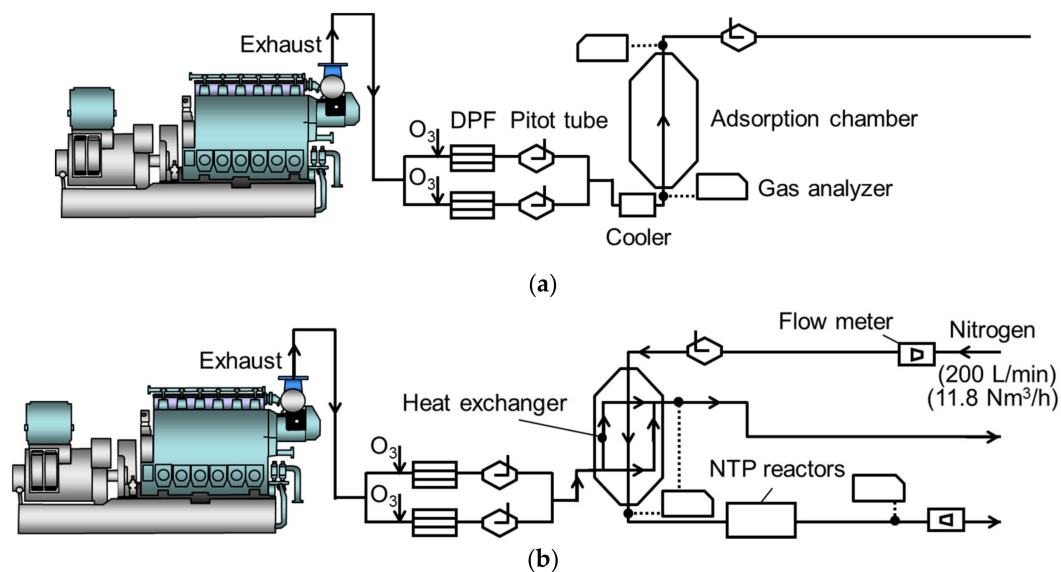

Figure 1. Process diagram of the NO_x reduction system for a marine diesel engine: (**a**) adsorption process; (**b**) desorption process.

3. Experimental Apparatus

A photograph of the diesel engine (6DK-20e, Daihatsu Diesel MFG Co. Ltd., Japan) is shown in Figure 2. Experiments are performed using an electrical sub-power generation marine engine bench in the laboratory. Table 1 shows the specifications of the engine. The specifications are four strokes, six cylinders with a cylinder bore of 200 mm and a stroke of 300 mm, and a constant rotation rate of 900 rpm. Table 2 shows the operating conditions. The maximum (100%) output power is 1071 kW. The fuel was marine diesel oil (A-heavy oil (the same grade as marine diesel oil), sulfur content = 0.075 mass%,

nitrogen content = 0.01 mass%, heating value = 45.4 MJ/kg). The exhaust flow rate was 3920 Nm^3/h for 50% load or output power, 5526 Nm^3/h for 75%, and 6815 Nm^3/h for 100% (N denotes the standard state of 0 °C, 0.1 MPa) [2].

Figure 2. Photograph of the targeted marine diesel engine (6DK-20e, maximum power = 1071 kW).

Table 1. Specifications of the marine diesel engine (6DK-20e).

Specification	Value
Number of Cylinders	6
Bore, mm	200
Stroke of cylinder, mm	300
Rotating speed, rpm	900
Weight of engine with a dynamo, tons	16

Table 2. Operating conditions of the marine diesel engine (6DK-20e).

Specification	Value	Value	Value
Load, %	100	75	50
Power, kW	1071	803	536
Exhaust gas flow, Nm^3/h	6815	5526	3920
Air flow rate from supercharger, Nm^3/kWmh	6.36	6.88	7.32
Exhaust gas components			
NO_x, ppm	780	710	660
CO, ppm	105	63	33
CO_2, %	5.4	4.9	4.8
O_2, %	13.6	14.2	14.4
HCs, ppm	120	120	120

Figure 3 shows a schematic of the experimental setup for the aftertreatment for the marine diesel engine. Figure 4 shows the experimental setup for exhaust-gas aftertreatment in the marine diesel engine system. Approximately 16% of the bypassed exhaust gas passes into a 150A pipe (in Japanese Industrial Standards; inner diameter = 155.2 mm) and through a set of ceramic DPFs (material: SiC, TYK

Corporation, Japan). Here, most of the PM is removed. Subsequently, the flow velocity is measured by a set of pitot tubes (L type, FV-21A, OKANO WORKS, Ltd. Japan). The accumulated PM in the DPF is treated using NTP-induced ozone (O_3) injection technology, as we previously reported [2,31]. After the PM removal, the NO_x in the exhaust gas is treated via adsorption and desorption processes with NTP in the same way as the previous experiment [2] as well as the measurements. The concentration of untreated NO_x from the engine is 400-760 ppm, and the ratio of NO_2/NO_x is approximately 15%. N_2 gas at a low flow rate in the desorption process is 11.8 Nm^3/h (200 L/min at 5 °C). A significantly higher concentration (typically 3660-25,000 ppm) of NO_x compared with that of the previous study (typically 4000 ppm) [2] flows out of the chamber and enters the NTP reactors, with a total energy consumption of 12.0 kW. NO_x is reduced into N_2 and O_2 according to reaction (1). As the upper limit of the analyzer is 2500 ppm, high-concentration desorbed NO_x gas in excess of 2500 ppm is diluted with atmospheric air. The actual NO_x concentration is estimated by comparing the O_2 concentration of the diluted exhaust gas with that of the raw exhaust.
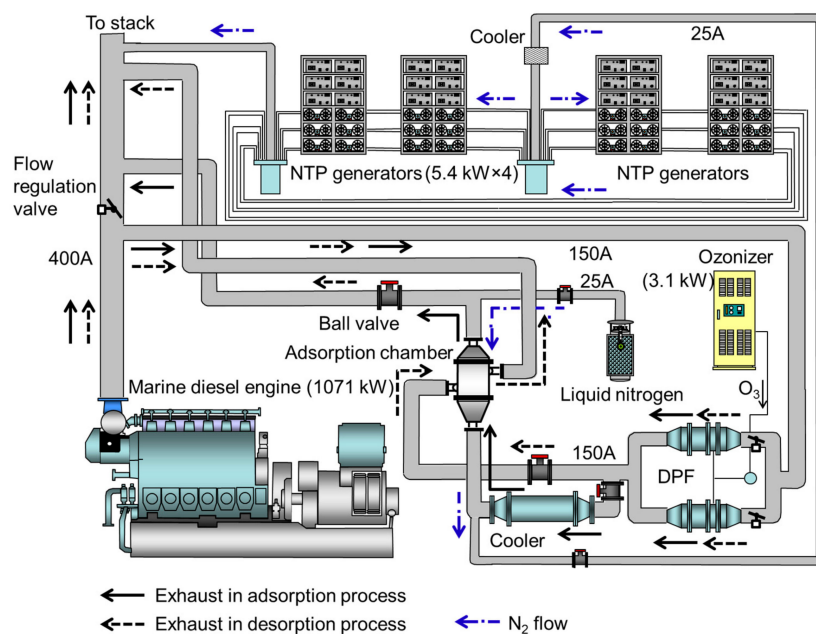

Figure 3. Schematic of the experimental setup for exhaust-gas aftertreatment in the marine diesel engine.
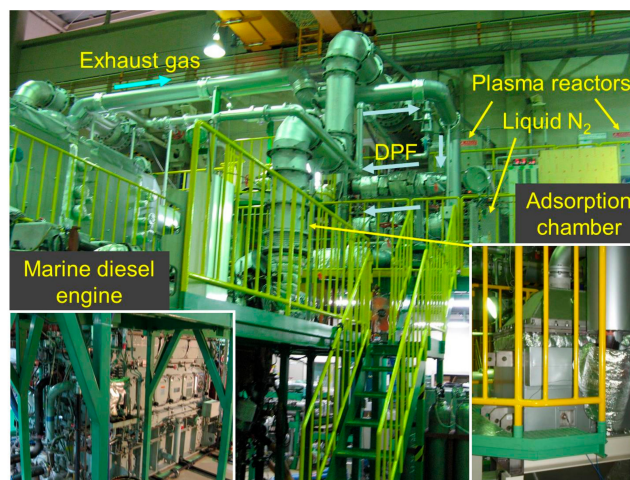

Figure 4. Photograph of the experimental setup for exhaust-gas aftertreatment in the marine diesel engine system.

Figure 5 shows the adsorption chamber equipped with a waste-heat exchanger that is specially designed and manufactured by Sumitomo Precision Products Co. Ltd. (type: XS6083). The directions of gas flow and the dimensions are shown. The same chamber that was used in a previous experiment is employed [2]. The adsorption chamber is designed optimally based on our results of the laboratory-scale experiment [25] and the previous pilot-scale ones [2,3]. The amount of packed adsorbent pellets is 80 kg, which represents 101 L by volume. Compared with the previous study [3], the dimensions of the chamber are different, and the cross-sectional area is 3.9 times larger. However, the vertical length is 0.7 times shorter. The volume of the adsorption chamber including relevant externals is approximately 0.5 m^3, which is smaller than the typical volume of 6.0 m^3 of a urea-solution tank. The mass of the adsorbent chamber without adsorbents is almost equal to that of empty urea-solution tank. Figure 5a shows a cross section of the chamber with two types of flow paths—flow path I (the number is 47, and each gap is 3.2 mm) and flow path II (the number is 48, and each gap is 8.9 mm)—alternately stacked inside. Figure 5b shows a side view of flow path I, in which the hot exhaust gas flows. Flow path I is empty, and flow path II is packed with adsorbent pellets, as shown in Figure 5c. In the adsorption process, while exhaust gas flows from the bottom inlet to the top outlet of flow path II, NO$_x$ is adsorbed onto the pellets. In the desorption process, heated exhaust gas travels along flow path I to heat the adsorbent pellets. Simultaneously, N$_2$ gas from a liquid N$_2$ cylinder flows from the top inlet to the bottom outlet of flow path II at a low flow rate to achieve O$_2$-lean condition, as shown in Figure 5b,c. Switching between these two processes is performed by opening and shutting the ball valves. The adsorbent used in this study is a MnO$_x$–CuO oxidative compound (N-140, 1.2–2.4 mm-sized granular pellets, Süd-Chemie Catalysts Japan, Inc.). The measurement points for the adsorbent temperature are shown in Figure 5c. The temperatures measured at these points are averaged for evaluating the efficiencies.
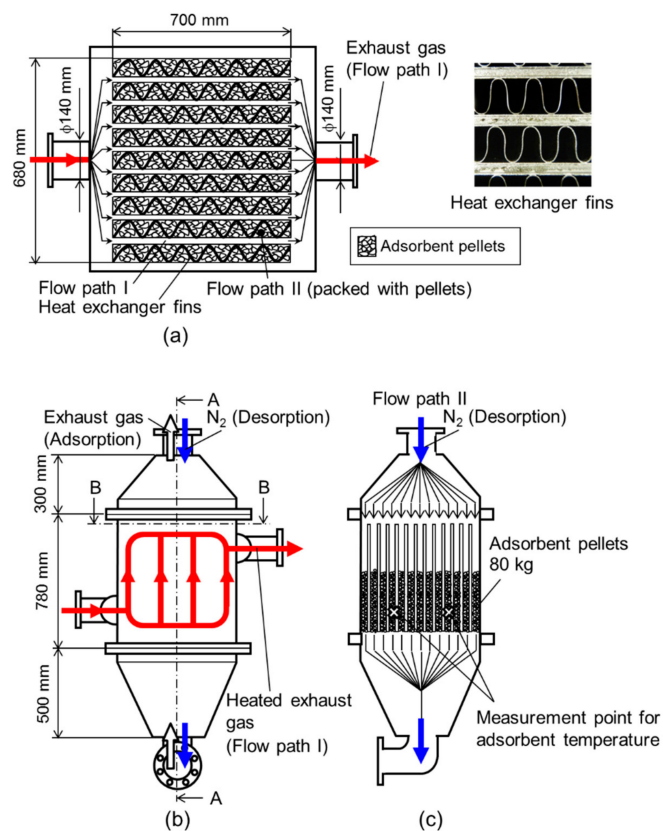

Figure 5. Schematic of the adsorption chamber containing 80 kg of adsorbents with gas flows in the desorption process. (**a**) Cross section B-B; (**b**) Side view; (**c**) Cross section A-A;

Table 3 presents the design specifications of the adsorption chamber. A counter-flow-type heat exchanger is used in the adsorption chamber. The design specifications are the same as those used in a previous study [2]. Thus, the total heat-exchange quantity is 61.2 kW. The pressure drop and space velocity are also presented in the table. When the amount of packed adsorbent pellets is 40 kg, the space velocity is higher than that in our previous study [3], with a ratio of 1.96 (i.e., 16,000/8150). Figure 6 shows a photograph and schematic of the NTP reactor used for reducing NO_x. The reactor consists of a surface-discharge element (ET-OC70G-C, Masuda Research Inc., Japan), air-cooling fins, and a flange to fix the discharge element to the frame. The structure of surface discharge is also presented in the figure. As shown, NO_x in the N_2 gas flows on the surface-discharge element. NO_x is reduced to the clean gases of N_2 and O_2 with the surface discharge plasma. The surface-discharge element is cooled with an air-cooling fan. The specifications of one unit of the NTP generator in Figure 3, which includes the power supplies and the NTP reactors, are as follows. Two of these reactors are powered by a single-pulse high-voltage power supply (HCII-70/2, Masuda Research Inc.). The maximum peak-to-peak voltage is 10 kV, with a frequency of 10 kHz. The maximum input power is $450 \times 2 = 900$ W. A unit of the NTP generator (HCII-OC70×12) consists of 12 NTP reactors and six power supplies. The total input power of a unit is 900 W × 6 = 5.4 kW, and the discharge power is 5.0 kW.

Table 3. Specifications of the adsorption chamber.

| Specification	Value
Operation Gauge Pressure	0.1 MPa
Heatproof temperature	300 ºC
Material of heat-exchanger fin	Stainless steel
Area and type of heat-exchanger fin Flow path I Flow path II	55 m², serrated fin 72 m², plain fin
Mass of adsorbent chamber without adsorbent pellets	920 kg
Amount and volume of packed adsorbent pellets	80 kg, 101 L
Pressure drop in adsorption process with adsorbent pellets (80 kg)	2 kPa (Load 75%, 810 Nm³/h)
Space velocity (exhaust gas: 800 Nm³/h, 175 °C; adsorbents: 80 kg)	16,000/h
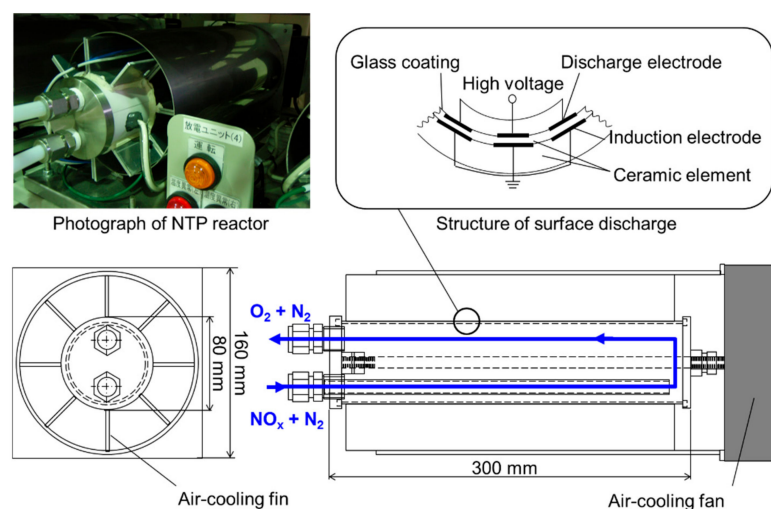
Figure 6. Schematic of the nonthermal plasma (NTP) reactor, showing the structure of the discharge section, along with a photograph of the NTP reactor.

4. Results and Discussion

Experiments are performed for 19 operation cycles. The NO_x reduction performance in the aftertreatment is evaluated. The engine operation was stopped once during each process.

Figure 7 shows the time-dependent NO_x emissions before and after the gas passes through the aftertreatment for cycles 16–19. Cycles 16–19 represent the transition of the adsorbent from the unsteady state to the steady state. The engine load is set as 75% for all adsorption processes and 50% for all desorption processes, considering the exhaust-gas temperatures for the adsorption and desorption of NO_x. This setting of the engine load is chosen to investigate the performance in a severe condition because it gives the severe condition for the aftertreatment, that is, high concentration of NO_x in adsorption and lower temperature in desorption processes. The amount of adsorbent pellets in the adsorption chamber is 80 kg. The mass flow rate for NO_x, which is shown on the vertical axis in Figure 7, is evaluated according to the molecular mass of NO_2, with the unit of $g(NO_2)/h$. Untreated NO_x in the adsorption process is represented by white circles with lines. Treated NO_x is represented by black circles with lines. NTP is applied only in the desorption processes, and the input power to the NTP generator is 12.0 kW. The mass flow rate of NO_x in the untreated exhaust gas is 1330–1500 $g(NO_2)/h$ in the steady state of engine operation. The engine operation is stopped at $t = 3900$ min in the adsorption process of cycle 17 and at $t = 4192$ min in the adsorption process of cycle 18. Each stoppage lasts for approximately half a day. It is noted that the difference in the duration of the desorption is just due to the engine operation timing. In the adsorption processes, the mass flow rate of NO_x decreases to 970–1280 $g(NO_2)/h$. In the desorption processes, the maximum concentrations of desorbed NO_x are 8180, 11,380, 3660, and 17,830 ppm in cycles 16–19, respectively. On average, 49% of the desorbed NO_x is reduced by the application of NTP. For example, considering cycle 19 in the graph, similar to the previous report [2], the hatched area represents the total mass of adsorbed NO_x, and the area in the desorption process represents the total mass of NO_x reduced by the NTP. The desorption of NO_x is enhanced in cycle 19.
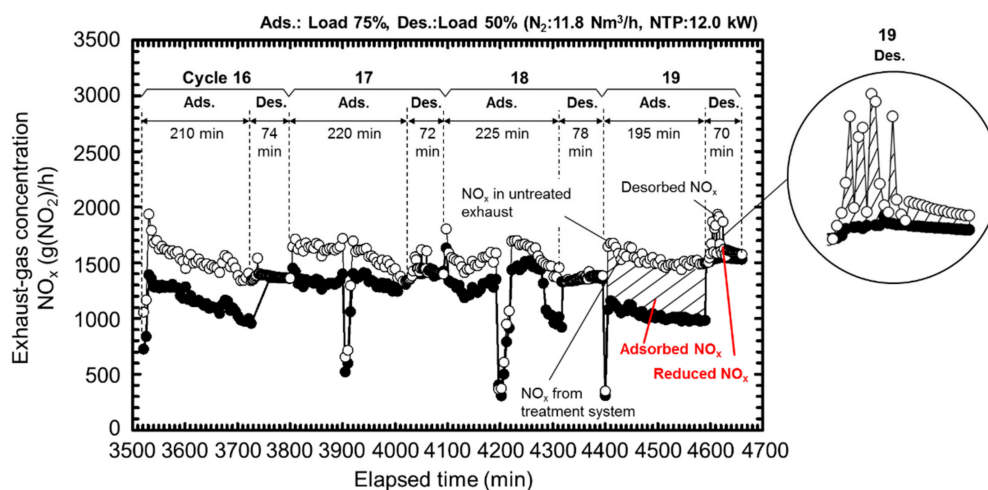

Figure 7. Time-dependent NO_x emissions before and after the gas passes through the aftertreatment for operation cycles 16–19.

Figure 8 shows the time-dependent temperature of the adsorbent pellets in cycles 16–19. At the beginning of each adsorption process, the adsorbent temperature is high because of residual heat from the previous desorption process. However, the temperature rapidly decreases to 50 °C under cooling. The exhaust gas is exceptionally uncooled at the beginning and is cooled at $t = 3606$ min in the adsorption process of cycle 16. Therefore, the temperature of the adsorbent pellets is high and becomes constant at $t = 3606$ min in cycle 16. The temperature decreases at $t = 3900$ min in the adsorption process of cycle 17 and at $t = 4192$ min in the adsorption process of cycle 18 because the engine is

stopped for approximately half a day. Consequently, the appropriate temperatures are achieved for both the adsorption and desorption processes.
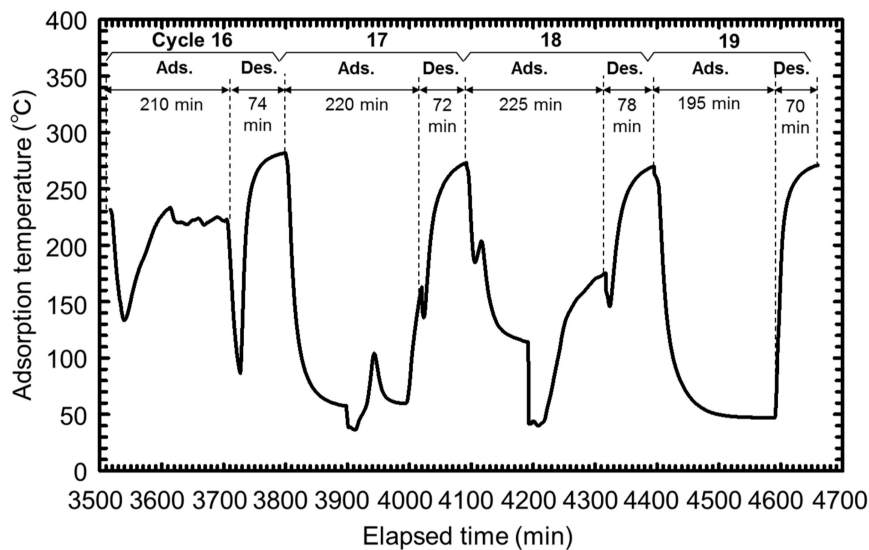

Figure 8. Time-dependent temperature in the adsorption chamber packed with 80 kg of adsorbent pellets in cycles 16–19.

Table 4 shows the resulting adsorbed, desorbed, reduced, and treated amounts of NO_x in cycles 16–19, as well as the gaseous flow rates and energy efficiencies in aftertreatment. The adsorbed mass of NO_x, W_a, ranges from 855 to 1651 g(NO_2). The desorbed mass of NO_x, W_d, ranges from 41.4 to 160 g(NO_2). The mass of NO_x reduced by the application of NTP, W_{NTP}, is in the range of 17.3–114 g(NO_2). The total amount of NO_x removed by the system is calculated as

$$W_{system} = W_a - W_d + W_{NTP} \tag{2}$$

The energy efficiency of the NTP treatment, which shows how to efficiently treat a mass of NO_x per unit of energy, is calculated as follows.

$$\eta_{NTP} = \frac{W_{NTP}}{E_{NTP}} \tag{3}$$

where, E_{NTP} represents the applied NTP energy. η_{NTP} is determined to be 1.1–8.1 g(NO_2)/kWh. The NO_x removal energy efficiency of the system is calculated as

$$\eta_{system} = \frac{W_{system}}{E_{NTP}} \tag{4}$$

The present technology exhibits the highest system energy efficiency, i.e., $\eta_{system} = 115$ g(NO_2)/kWh, in cycle 19. The low NTP power of 12.0 kW contributes to this high efficiency. In the adsorption process of cycle 19, the typical concentrations of gaseous NO_2, NO, CO, and O_2 downstream of the adsorption chamber are 100 ppm, 430 ppm, 69 ppm, and 13.9%, respectively. In the desorption process of cycle 19, the NO_x concentrations upstream and downstream of the NTP generator are 5610 and 1620 ppm, respectively.

Figure 9 shows the relationship between the mass of desorbed NO_x and the reduction energy efficiency in the NTP treatment in the desorption processes of cycles 16–19. The data for the desorption processes of cycles 5–12 of the previous experiments [2] are also shown. Cycles 13–15 are not shown, because NO_x reduction via NTP is not performed. The data plots are presented with the time period of the desorption process. The relationship between the reduction and the mass of desorbed NO_x is approximately given by the line of

$$\eta_{\text{NTP}} = 0.0442 W_{\text{d}}. \tag{5}$$

The coefficient, 0.0442, is improved compared with that reported in the previous study [2], because it is determined using a larger amount of data in repeated experiments. Furthermore, a high reduction efficiency of 71% is achieved in cycle 19 for the discharge power of 12.0 kW. The efficiency of reduction via NTP, η_{re}, is defined as the ratio of the amount of reduced NO_x to the amount of desorbed NO_x:

$$\eta_{\text{re}} = W_{\text{NTP}}/W_{\text{d}} \times 100. \tag{6}$$

Table 4. Treated NO_x amount and removal energy efficiency (g(NO_2)/kWh) in cycles 16–19.

| Cycle	16	17	18	19
Averaged flow rate of exhaust gas, Nm^3/h	944	999	948	946
(1) Adsorbed, W_{a}, g(NO_2)	1248	855	937	1651
(2) Desorbed, W_{d}, g(NO_2)	49.9	113	41.4	160
(3) Reduced by NTP, W_{NTP}, g(NO_2)	26.0	35.4	17.3	114
(4) Removed in system, W_{system}, g(NO_2) $W_{\text{system}} = W_{\text{a}} - W_{\text{d}} + W_{\text{NTP}}$	1224	777	913	1605
NTP power, kW	12.0	12.0	12.0	12.0
NTP energy, E_{NTP}, kWh	14.8	14.4	15.6	14.0
$\eta_{\text{NTP}} = W_{\text{NTP}}/E_{\text{NTP}}$, g($NO_2$)/kWh	1.8	2.5	1.1	8.1
$\eta_{\text{system}} = W_{\text{system}}/E_{\text{NTP}}$, g($NO_2$)/kWh	82.7	54.0	58.5	115
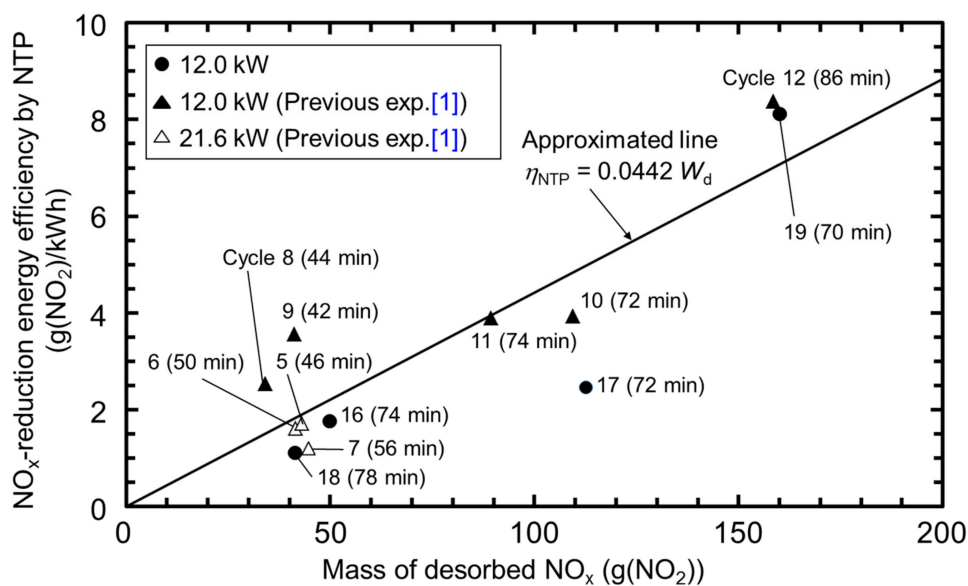
Figure 9. Relationship between the energy efficiency of NO_x reduction via NTP and the mass of desorbed NO_x from the adsorbent in the adsorption process with 80 kg of adsorbent pellets.

The system energy efficiency of $\eta_{\text{system}} = 115$ g(NO_2)/kWh is lower than $\eta_{\text{system}} = 161$ g(NO_2)/kWh observed in the previous study [2]. This is because the previous investigation is performed by exploiting the high-adsorption performance of relatively new adsorbents. However, the present study is conducted in the steady state of the adsorption and desorption of NO_x, in which the adsorption performance decreases. However, the desorption performance and efficiency of NO_x reduction via NTP are higher those in the previous study. For a marine diesel engine with a rotation speed of 900 rpm, NO_x emissions should be reduced by 6.89 g/kWh to satisfy the IMO emission standards from Tier II to

III. The recorded energy efficiency of the system (η_{system} = 115 g(NO_2)/kWh) corresponds to only 6.0% (6.89/115 × 100) of the engine output power satisfying the requirement. Thus, the high-performance aftertreatment using the present technology satisfies the most recent IMO emission standards.

5. Conclusions

A pilot-scale aftertreatment technology for NO_x reduction in marine diesel exhaust gas was developed. An experiment using a marine diesel engine (output power of 1 MW) was conducted using an NTP generator with a power of 12.0 kW for a larger number of cycles compared with our previous study. The amount of adsorbents was 80 kg. The characteristics of NO_x adsorption/desorption and the NO_x reduction efficiencies were analyzed according to experimental data. The experiments were repeated for up to 19 cycles (longer period than the previous study). Significantly more data were obtained to increase the accuracy for estimating the efficiency of NO_x reduction via NTP. A high reduction efficiency of 71% was achieved using NTP. Additionally, the technology exhibited a high system energy efficiency of 115 g(NO_2)/kWh for NO_x removal. Given that a high-concentration NO_x was treated by NTP after NO_x adsorption and desorption from adsorbents, the present aftertreatment can simultaneously achieve high reduction and energy efficiencies. This high efficiency satisfies the most recent requirement of NO_x reduction of 6.89 g/kWh based on the IMO emission standards from Tier II to III for a marine diesel engine with a rotation speed of 900 rpm [2]. Thus, the efficient aftertreatment technology requires only 6.0% of the engine output power. The present aftertreatment technology can satisfy the same-level requirement in the future. Because this aftertreatment technology does not use any rare or precious-metal catalysts, harmful ammonia, or a urea-solution storage tank inside the ship, it has significant advantages compared with conventional exhaust-gas treatments, such as the marine SCR method.

Conflicts of Interest: The authors declare no conflicts of interest.

References

1. Okubo, M.; Kuwahara, T. *New Technologies for Emission Control in Marine Diesel Engines*; Elsevier: Oxford, UK, 2019; ISBN 978-0-12-812307-2.
2. Kuwahara, T.; Yoshida, K.; Kuroki, T.; Hanamoto, K.; Sato, K.; Okubo, M. Pilot-Scale Aftertreatment Using Nonthermal Plasma Reduction of Adsorbed NO_x in Marine Diesel-Engine Exhaust Gas. *Plasma Chem. Plasma Process.* **2014**, *34*, 65–81. [CrossRef]
3. Kuwahara, T.; Yoshida, K.; Hanamoto, K.; Sato, K.; Kuroki, T.; Okubo, M. A Pilot-Scale Experiment for Total Marine Diesel Emission Control Using Ozone Injection and Nonthermal Plasma Reduction. *IEEE Trans. Ind. Appl.* **2015**, *51*, 1168–1178. [CrossRef]
4. Grados, C.V.D.; Uriondo, Z.; Clemente, M.; Espadafor, F.J.J.; Gutiérrez, J.M. Correcting Injection Pressure Maladjustments to Reduce NO_x Emissions by Marine Diesel Engines. *Transp. Res. Part. D Transp. Environ.* **2009**, *14*, 61–66. [CrossRef]
5. Forzatti, P. Present Status and Perspectives in De-NO_x SCR Catalysis. *Appl. Catal. A Gen.* **2001**, *222*, 221–236. [CrossRef]
6. Kang, M.; Park, E.D.; Kim, J.M.; Yie, J.E. Cu–Mn Mixed Oxides for Low Temperature NO Reduction with NH3. *Catal. Today* **2006**, *111*, 236–241. [CrossRef]

7. Gómez-García, M.A.; Zimmermann, Y.; Pitchon, V.; Kiennemann, A. Multifunctional Catalyst for De-NO$_x$ Processes: The Selective Reduction of NO$_x$ by Methane. *Catal. Commun.* **2007**, *8*, 400–404. [CrossRef]

8. Cheng, X.; Bi, X.T. A Review of Recent Advances in Selective Catalytic NO$_x$ Reduction Reactor Technologies. *Particuology* **2014**, *16*, 1–18. [CrossRef]

9. Kwon, D.W.; Nam, K.B.; Hong, S.C. The Role of Ceria on the Activity and SO$_2$ Resistance of Catalysts for the Selective Catalytic Reduction of NO$_x$ by NH$_3$. *Appl. Catal. B Environ.* **2015**, *166*, 37–44. [CrossRef]

10. Boscarato, I.; Hickey, N.; Kašpar, J.; Prati, M.V.; Mariani, A. Green Shipping: Marine Engine Pollution Abatement Using a Combined Catalyst/Seawater Scrubber System. 1. Effect of Catalyst. *J. Catal.* **2015**, *328*, 248–257. [CrossRef]

11. Da Cunha, B.N.; Gonçalves, A.M.; da Silveira, R.G.; Urquieta-González, E.A.; Nunes, L.M. The Influence of a Silica Pillar in Lamellar Tetratitanate for Selective Catalytic Reduction of NO$_x$ Using NH$_3$. *Mater. Res. Bull.* **2015**, *61*, 124–129. [CrossRef]

12. McAdams, R.; Beech, P.; Shawcross, J.T. Low Temperature Plasma Assisted Catalytic Reduction of NO$_x$ in Simulated Marine Diesel Exhaust. *Plasma Chem. Plasma Process.* **2008**, *28*, 159–171. [CrossRef]

13. Wang, H.; Li, X.; Chen, P.; Chen, M.; Zheng, X. An Enhanced Plasma-Catalytic Method for DeNO$_x$ in Simulated Flue Gas at Room Temperature. *Chem. Commun.* **2013**, *49*, 9353–9355. [CrossRef] [PubMed]

14. Jõgi, I.; Stamate, E.; Irimiea, C.; Schmidt, M.; Brandenburg, R.; Hołub, M.; Bonisławski, M.; Jakubowski, T.; Kääriäinen, M.-L.; Cameron, D.C. Comparison of Direct and Indirect Plasma Oxidation of NO Combined with Oxidation by Catalyst. *Fuel* **2015**, *144*, 137–144. [CrossRef]

15. Pietikäinen, M.; Väliheikki, A.; Oravisjärvi, K.; Kolli, T.; Huuhtanen, M.; Niemi, S.; Virtanen, S.; Karhu, T.; Keiski, R.L. Particle and NO$_x$ Emissions of a Non-Road Diesel Engine with an SCR Unit: The Effect of Fuel. *Renew. Energy* **2015**, *77*, 377–385. [CrossRef]

16. Guo, M.; Fu, Z.; Ma, D.; Ji, N.; Song, C.; Liu, Q. A Short Review of Treatment Methods of Marine Diesel Engine Exhaust Gases. *Procedia Eng.* **2015**, *121*, 938–943. [CrossRef]

17. Manivannan, N.; Agozzino, G.; Balachandran, W.; Abbod, M.F.; Jayamurthy, M.; Natale, F.D.; Brennen, D. NO Abatement Using Microwave Micro Plasma Generated with Granular Activated Carbon. *IEEE Trans. Ind. Appl.* **2017**, *53*, 5845–5851. [CrossRef]

18. Madhukar, A.; Rajanikanth, B.S. Augmenting NO$_x$ Reduction in Diesel Exhaust by Combined Plasma/Ozone Injection Technique: A Laboratory Investigation. *High. Volt.* **2018**, *3*, 60–66. [CrossRef]

19. Hołub, M.; Kalisiak, S.; Borkowski, T.; Myśków, J.; Brandenburg, R. The Influence of Direct Non-Thermal Plasma Treatment on Particulate Matter (PM) and NO$_x$ in the Exhaust of Marine Diesel Engines. *Pol. J. Environ. Stud.* **2010**, *19*, 1199–1211.

20. Hołub, M.; Borkowski, T.; Jakubowski, T.; Kalisiak, S.; Myśków, J. Experimental Results of a Combined DBD Reactor-Catalyst Assembly for a Direct Marine Diesel-Engine Exhaust Treatment. *IEEE Trans. Plasma Sci.* **2013**, *41*, 1562–1569. [CrossRef]

21. Schmidt, M.; Basner, R.; Brandenburg, R. Hydrocarbon Assisted NO Oxidation with Non-Thermal Plasma in Simulated Marine Diesel Exhaust Gases. *Plasma Chem. Plasma Process.* **2013**, *33*, 323–335. [CrossRef]

22. Seddiek, I.S.; Elgohary, M.M. Eco-Friendly Selection of Ship Emissions Reduction Strategies with Emphasis on SO$_x$ and NO$_x$ Emissions. *International J. Nav. Archit. Ocean. Eng.* **2014**, *6*, 737–748. [CrossRef]

23. Han, Z.; Liu, B.; Yang, S.; Pan, X.; Yan, Z. NO$_x$ Removal from Simulated Marine Exhaust Gas by Wet Scrubbing Using NaClO Solution. *J. Chem.* **2017**, *2017*, 9340856. [CrossRef]

24. Yoshida, K.; Kuroki, T.; Okubo, M. Diesel Emission Control System Using Combined Process of Nonthermal Plasma and Exhaust Gas Components' Recirculation. *Thin Solid Films* **2009**, *518*, 987–992. [CrossRef]

25. Kuwahara, T.; Yoshida, K.; Kannaka, Y.; Kuroki, T.; Okubo, M. Improvement of NO$_x$ Reduction Efficiency in Diesel Emission Control Using Nonthermal Plasma Combined Exhaust Gas Recirculation Process. *IEEE Trans. Ind. Appl.* **2011**, *47*, 2359–2366. [CrossRef]

26. Okubo, M.; Tanioka, G.; Kuroki, T.; Yamamoto, T. NO$_x$ Concentration Using Adsorption and Nonthermal Plasma Desorption. *IEEE Trans. Ind. Appl.* **2002**, *38*, 1196–1203. [CrossRef]

27. Okubo, M.; Inoue, M.; Kuroki, T.; Yamamoto, T. NO$_x$ Reduction after Treatment System Using Nitrogen Nonthermal Plasma Desorption. *IEEE Trans. Ind. Appl.* **2005**, *41*, 891–899. [CrossRef]

28. Yoshida, K.; Okubo, M.; Yamamoto, T. Distinction between Nonthermal Plasma and Thermal Desorptions for NO$_x$ and CO$_2$. *Appl. Phys. Lett.* **2007**, *90*, 131501. [CrossRef]

29. Yoshida, K.; Okubo, M.; Kuroki, T.; Yamamoto, T. NO$_x$ Aftertreatment Using Thermal Desorption and Nitrogen Nonthermal Plasma Reduction. *IEEE Trans. Ind. Appl.* **2008**, *44*, 1403–1409. [CrossRef]

30. Okubo, M.; Yamamoto, Y.; Kuroki, K. Exhaust Gas Cleaning Method and System. Japan Patent No. 2003-361010, 21 October 2003.

31. Kuwahara, T.; Yoshida, K.; Hanamoto, K.; Sato, K.; Kuroki, T.; Yamamoto, T.; Okubo, M. Pilot-Scale Experiments of Continuous Regeneration of Ceramic Diesel Particulate Filter in Marine Diesel Engine Using Nonthermal Plasma-Induced Radicals. *IEEE Trans. Ind. Appl.* **2012**, *48*, 1649–1656. [CrossRef]